

Evaluation of Subacute and Chronic Cryotherapy Lesions Using Histopathology and Contrast Enhanced MR Images in the Dog Prostate Model

D. M. Bouley¹, E. Liu², K. Butts Pauly², M. Van den Bosch², and B. Daniel²

¹Comparative Medicine, Stanford University, Stanford, CA, United States, ²Radiology, Stanford University, Stanford, CA, United States

Introduction

Minimally invasive thermal-based treatments, such as cryosurgery, are suitable options for the treatment of BPH or prostate cancer. Our radiologists use MRI to monitor delivery of this treatment in a canine prostate model and use contrast enhanced (CE) T1-weighted images compared with the histopathology of acute lesions in order to better predict the extent of target tissue ablation *in vivo*. In this study, we created cryolesions using two different treatment protocols and analyzed the lesions at three different post-treatment intervals with CE MR images and histopathology in order to understand the MRI appearance of subacute to chronic lesions and the potential for tissue regeneration in the prostate.

Methods

Three adult male beagles were anesthetized and placed in the 0.5T Signa open MRI system. Cryolesions were created in each prostate using 17 g cryoprobes, and two treatment protocols: Protocol A (PA) - 1 probe inserted in the left side and lethal tissue damage created with a final temperature < -40°C, and two freeze-thaw cycles, and Protocol B (PB) - two probes inserted in the right with sublethal tissue damage created with a final temperature between 0°C and -10°C, and one freeze-thaw cycle. A total of 6 cryolesions were created bilaterally in the 3 canine prostates. The sizes of the acute cryolesions were measured with CE T1-weighted images after administration of gadolinium. All dogs were recovered from anesthesia with no peri-procedural complications. At the end of each different post-treatment interval, each dog was re-anesthetized, the prostate lesions evaluated with CE T1-weighted images, and euthanized. Dog 1 was sacrificed after 4 days, dog 2 after 14 days, and dog 3 after 53 days. The prostates were excised, sliced and photographed. The sections were incubated in 1% triphenyl, tetrazolium chloride (TTC) for 20 minutes at 37°C, photographed, transferred to 10% buffered neutral formalin, processed for routine paraffin embedding, and stained with hematoxylin and eosin (H&E) and a Trichrome stain. Some slides were scanned by CLARiENT, Inc. for digital analysis.

Results

Post-treatment CE images of the acute cryolesions demonstrated large non-enhancing areas surrounded by an enhancing rim. Lesions created with PA were consistently larger and less enhanced than the lesions created with PB. Pre-euthanasia images revealed marked shrinkage in lesion size and gradual reduction in non-enhanced areas (Fig. 1 A, B). At necropsy, periprostatic fat was adhered to the capsule and at each progressive time point, the contours of the prostate capsules overlying the treatment sites were more depressed. On cut surface, lesions were dark red/purple with sharply demarcated borders (Fig. 1 C). Histology of the PA lesion in the prostate of dog 1, 4 days post treatment, showed a large central area of hemorrhage and gland necrosis surrounded by a narrow rim of regenerative glands, mild mixed inflammation, neocapillary and fibroblast proliferation. The PB lesion had minimal central necrosis and a wide rim of regeneration (Figs. 1 D-F). In dogs 2 and 3, PB lesions could not be distinguished with CE images, and PA lesions had become significantly contracted. Histologically, PB lesions consisted almost entirely of regenerated glands embedded in immature collagen or granulation tissue (Fig. 1 G), whereas PA lesions had central regions of very dense fibrosis with very few glands (Fig. 1 H), and were surrounded by large areas of less mature regeneration similar to PB lesions.

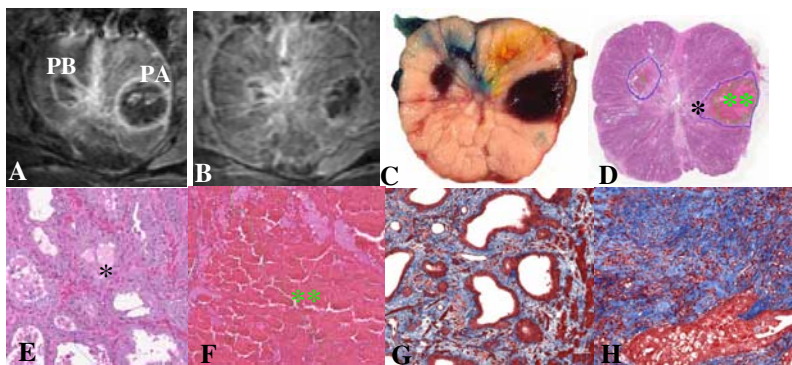


Figure 1. A) CE image of dog 1, at the time of treatment. The lesion created by PA is on the image right (animal left) and by PB is on the image left (animal right). Locations of the lesions are the same in images B-D. B) CE image of dog 1, 4 days later – note shrinkage in lesions. C) Fresh tissue slice corresponding with image B. D) Subgross histological view of the tissue depicted in C. The outer boundaries of the lesion are outlined in blue and the inner, more lethally damaged tissues are outlined in green E) Regeneration of glands at the outer edge of the lesion in image D (*). F) Necrosis and hemorrhage in the middle of the lesion (**). G) Fibrosis and gland regeneration in dog 2, 14 days post-treatment with PB. H) Dense collagen and a regenerating gland in dog 2, 14 days post-treatment with PA. (D-F H&E stain, G-H Trichrome stain which shows collagen in blue.)

Conclusions

We have used the canine prostate cryoablation model to compare CE MR images with histopathology in order to provide verification of cell killing and overall treatment success. Evaluation of two different treatment protocols at three different intervals post treatment has provided valuable insight into the potential for the healing of cryolesions due to the significant regenerative capabilities of the prostate, suggesting the need for colder temperatures and increased freeze-thaw cycles in order to guarantee more complete ablation of the target tissue during initial treatment.

Acknowledgements

NIH R01 CA092061-01A2

References

Butts, K., JMRI, 2003,17:131-135, Coad, JE., Proc. SPIE, 2003, 2954:27-36.